Microchemical Journal 198 (2024) 110172

Contents lists available at ScienceDirect

Microchemical Journal

journal homepage: www.elsevier.com/locate/microc

Malachite green as a dual visual/electrochemical indicator for loop-mediated isothermal amplification: Application to SARS-CoV-2 detection

Pablo Rioboó-Legaspi [a], Noelia Rabanal-Rubio [a], Estefanía Costa-Rama [a,*], María Dolores Cima-Cabal [b], María del Mar García-Suárez [b], M. Teresa Fernández-Abedul [a,*]

[a] Departamento de Química Física y Analítica, Facultad de Química, Universidad de Oviedo, Spain
[b] Escuela Superior de Ingeniería y Tecnología, Universidad Internacional de La Rioja, Spain

ARTICLE INFO

Keywords:
Loop-mediated isothermal amplification (LAMP)
Nucleic acid amplification
Dual detection
Electrochemical detection (ED)
Screen-printed electrodes (SPEs)
Malachite green (MG)
SARS-CoV-2

ABSTRACT

Loop-mediated isothermal amplification (LAMP) has arisen as an outstanding molecular technique for the amplification of nucleic acids, becoming an important alternative to PCR due to its simplicity and high sensitivity. However, traditional visual readout used in LAMP only provides qualitative results and can thus not provide a precise quantification of the target DNA/RNA in the sample. To overcome this, electroactive reporters incorporated in the reaction mix can provide a subsequent quantitative result of the analysis. In this work, malachite green, a commonly used colorimetric LAMP indicator, is used as an electrochemical probe to obtain quantitative results. For this purpose, its optical and electrochemical behavior has been assessed for further use in LAMP detection. Using SARS-CoV-2 RNA as template, we have developed a quantitative detection method, proving the usefulness of this molecule as a dual optical/electrochemical indicator. Thereby, with the electrochemical detection using screen-printed electrodes on which a drop of the LAMP reaction is deposited, a calibration curve with a linear dynamic range comprised between 22 and 4296 copies/μL was achieved, with a practical limit of detection of 22 copies/μL. In this method, validated with clinical samples, malachite green is used, by the first time, as a dual visual electrochemical/visual probe that can provide both an initial visual qualitative assessment together with an electrochemical quantification.

1. Introduction

Quantitative polymerase chain reaction (qPCR) is the gold-standard for nucleic acid determination [1]. However, in an era where point-of-care (POC) diagnostics have become essential, this technique still presents some major inconveniences (e.g., the required instrumentation) that hamper its decentralization. Because of that, isothermal amplifications arise as an alternative with similar performance but simpler workflow. Out of all the possibilities, loop-mediated isothermal amplification (LAMP) can be considered as one of the most promising and robust amplification strategies. This is performed at *ca.* 65 °C, leading to large copy numbers in around 30 min, creating over 50-fold more amplicons compared to other PCR-based techniques [1]. However, conventional LAMP readouts rely on naked eye semiquantitative methods mainly based on color shifts, which require benchtop instrumentation when reliable quantification is required, making difficult analysis decentralization. To overcome this, electrochemical approaches provide sensitive alternatives for on-site analysis. They use simple and well-established materials and instrumentation, such as flat electrochemical cells (e.g., screen-printed electrodes, SPEs) and potentiostats, which can be pocket-sized and field deployable [2,3].

These electrochemical strategies rely on changes that happen along the LAMP reaction, such as DNA synthesis, pH drop or inorganic pyrophosphate release. Thus, direct approaches based on the change of conductivity and resistance [4] or pH [5,6] have been reported. The change with pH of the electrocatalytic effect of palladium nanoclusters on the oxygen reduction reaction has also been employed to detect LAMP reactions [7]. On the other hand, the use of electrochemical reporter molecules is the most common approach. They can be either free in the reaction medium, such as Hoechst-33258 [8], methylene blue [9], or ruthenium hexamine complex [10], or conjugated to DNA-probes as in the case of ferrocene-labelled [11] or methylene blue-labelled [12]

* Corresponding authors.
E-mail addresses: costaestefania@uniovi.es (E. Costa-Rama), mtfernandeza@uniovi.es (M.T. Fernández-Abedul).

https://doi.org/10.1016/j.microc.2024.110172
Received 3 November 2023; Received in revised form 13 February 2024; Accepted 14 February 2024
Available online 18 February 2024

DNA strands.

Complex approaches are noteworthy indeed, but additional reagents and steps complicate the workflow and increase overall cost and time. The optimal approach would be the use of indicators already present in commercial LAMP kits that could be also exploited as electrochemical reporters. In this context, phenol red (PR) has already been characterized and studied for use as dual optical/electrochemical indicator for the determination of *Streptococcus pneumoniae* DNA and SARS-CoV-2 RNA [14,15]. The use of this molecule does not change the workflow (since it is already contained in the kit) and can provide additional quantitative information. Furthermore, indicators are commonly present at high concentration, providing a precise and defined analytical signal.

Malachite green (MG) is a cationic dye, widely used as an antifungal and antiprotozoal compound for fish. It is used as colorimetric indicator for both LAMP-based sensing [13–16] and wearable disease sensing devices [17]: it shifts from clear to light blue as LAMP progresses, providing visual information about the process. MG has a pH-based color shift [18], interacting also with double-stranded DNA [19].

In this work we have studied the behavior of MG in LAMP reactions, evaluating the effect of different variables over its equilibrium. We have measured the changes both optically and electrochemically to define a dual visual/electrochemical reporter for quali/quantitative LAMP, providing a first visual result of the amplification and enabling a subsequent quantification via electrochemical measurement. The methodology has been applied to the detection of SARS-CoV-2 RNA via reverse transcriptase LAMP (RT-LAMP), as a model of pathogen producing infectious diseases, where sensitivity and *in-situ* analysis become relevant (Scheme 1).

2. Materials and methods

2.1. LAMP assay

The N1 fragment of the SARS-CoV-2 genome was amplified using LAMP primers based on sequences from previous studies [20]. Primer sequences and reagents for LAMP reaction can be found in supplementary material. The LAMP reactions were performed mixing 13.5 μL of Blue-LAMP RT KIT (CB) (including *Bst* 2.0 DNA Polymerase, a colorimetric indicator and 0.7 mM dUTG), 0.3 μL of 0.3 U UDG (Uracyl-DNA-Glycosylase), 2.5 μL of primer mix (1.6 μM each FIP and BIP primer, 0.2 μM each F3 and B3 primer and 0.4 μM each LoopF and LoopB primer), 7.7 μL of PCR-grade dH_2O, and 1 μL of template SARS-CoV-2 RNA (at the desired concentration) for positive reactions and 1 μL of PCR-grade dH_2O for negative (non-template) control reactions. All reactions were performed on low-retention, nuclease-free PCR grade tubes and under sterile conditions in a laminar flow hood. Reactions were incubated in a thermal cycler at 65 °C for 30 min, with a first 10-min step at 37 °C for UDG activity. To prevent carryover contaminations, all the equipment was cleaned with 5 % NaClO solution. Additionally, LAMP reactions and subsequent electrochemical measurements were performed in laboratories at different facilities to prevent carryover contaminations. Detailed reagents, materials, and equipment are included in the supplementary material.

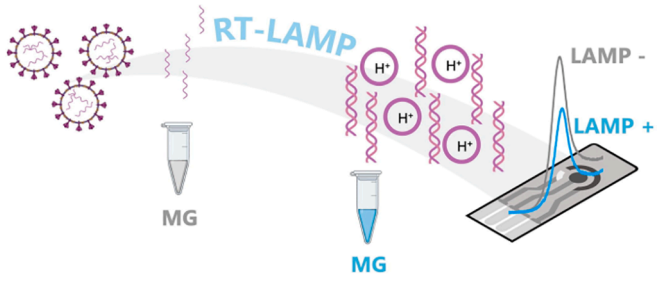

Scheme 1. Electrochemical LAMP methodology proposed in this work. SARS-CoV-2 RNA is amplified using RT-LAMP in the presence of malachite green, resulting in a shift from its clear to its blue form. This change in the form of MG results in a change in its electrochemical process that can be correlated with the copy number of the sample prior to its amplification.

2.2. Colorimetric detection of malachite green

The effect of different parameters associated with the progression of LAMP reactions (pH drop, temperature incubation, presence of DNA) was assessed using a solution of 100 μM MG (malachite green chloride) in 40 mM Tris-HCl buffer and Isothermal Amplification Buffer. Solutions were taken to the pH values considered for this study and, if needed, sheared salmon sperm DNA was also added to the desired concentration. Solutions were kept under dark storage to avoid MG photodegradation. For the study of the temperature effect, samples kept at room temperature and at LAMP temperature (30 min at 65 °C) were evaluated. Color shift was first evaluated visually and then using UV–VIS spectrophotometry. Detailed reagents, materials, and equipment are included in the supplementary material.

2.3. Electrochemical detection of malachite green

Commercial thick-film screen printed electrodes (SPEs, 27.5 x 10.1 x 0.35 mm, S1PE, Micrux® Technologies) were used for all electrochemical measurements. This SPE-based cell contains three electrodes, including a circle-shaped working electrode (WE) with a 3-mm diameter and a hook-shaped counter electrode (CE), both made of carbon ink, and a silver-ink pseudoreference electrode (RE). For the electrochemical measurements, 25 μL of the working solution or LAMP reaction were deposited over the SPE card, covering all three electrodes. Measurements were recorded at room temperature. To prevent MG photodegradation, the cell was kept away from light during the measurements. Each measurement required one three-electrode card, and cyclic voltammograms (CVs) and linear sweep voltammograms (LSV) were recorded by scanning at a scan rate of 0.05 $V{\cdot}s^{-1}$. Detailed reagents, materials, and equipment are included in the supplementary material.

2.4. Sample collection

Nasopharyngeal swab samples were collected at the Central University Hospital of Asturias (HUCA). Swabs were introduced in 500 μL of 10 mM Tris-EDTA (TE, pH 8.0) in microcentrifuge tubes. Samples were inactivated at 95 °C for 5 min [21]. This study was carried out in accordance with the recommendations of the Ethical Committee on Regional Clinical Research of the Principality of Asturias.

2.5. Statistics

Results in this study are represented as mean value ± standard deviation (SD). Differences between data groups were analyzed using Student's T-test (two-tailed, non-paired samples), prior test for normality and homogeneity of variance using the Shapiro-Wilk and Bartlett's test, respectively. Differences were considered statistically relevant at $p < 0.05$.

3. Results and discussion

3.1. Malachite green in LAMP reactions: Optical characterization

To understand the behavior of MG in LAMP solutions, an initial optical characterization of the color change of MG regarding other factors present in LAMP reactions was carried out. The first factor studied was the pH of the reaction. The color change of MG in aqueous solutions can be related to the change of pH in the solution, since protons are involved in the equilibrium established between the different MG forms

[22,23]. Starting at higher pH values, MG presents a first change from colorless to light blue (pK_a of 6.9) and a second one from light blue to green (pK_a of 2.0). As LAMP progresses, protons and inorganic pyrophosphate (PPi) are released to the medium, with nucleotide incorporation to the new DNA strand [18,20,22]. With that in mind, we expect the equilibrium shown in Fig. 1A to be the one involved in LAMP reactions, as the pH here spans between 8 and 6, approximately. This equilibrium has been thoroughly studied and is based on the change from the colorless neutral carbinol to the blue cationic dye [24]. For assessing the correlation of the MG color change with pH, we studied the behavior of 100 μM MG solutions in 0.1 M Tris-HCl buffer, the one used in LAMP reactions, at different pH values, ranging from 9.0 to 6.0.

From there on, and for each pH value, two assays were performed in parallel, one tube being left at room temperature and another one being subjected to a heat treatment simulating the one occurring in LAMP reactions (65 °C for 30 min). In this way, the role of temperature in color shift can be also evaluated. Results are shown in Fig. 1B. It must be noted that the initial color of all the solutions after MG addition was, regardless of its pH, dark blue. During the first 30 min, only a color shift was seen on those reactions incubated at 65 °C, in such a way that the blue became lighter for higher pH values. However, after 24 h a stable equilibrium was reached, as there was no color difference between heat-treated solutions and those at RT. At pH 9 the solution was colorless, due to the predominance of the carbinol form, and the subsequent pH values showing a deeper blue, indicating the presence of the cationic form. Absorbance values for different pH and temperature treatment are shown in Fig. S1A.

From this study we can first infer the importance of the heat treatment in the time for MG to reach the equilibrium with its final color form. Incubation at 65 °C during 30 min clearly favors the establishment of the equilibrium. According to the initial pH of LAMP reactions, the carbinol form of the MG indicator is the predominant; therefore, solutions should be colorless. A shift to blue happens when amplification occurs [13–16].

Additionally, MG interacts with double stranded DNA (dsDNA), which has already been demonstrated optically and electrochemically. MG interacts both electrostatically with the DNA backbone and via intercalation due to its planar structure [19]. The hypochromic effect of

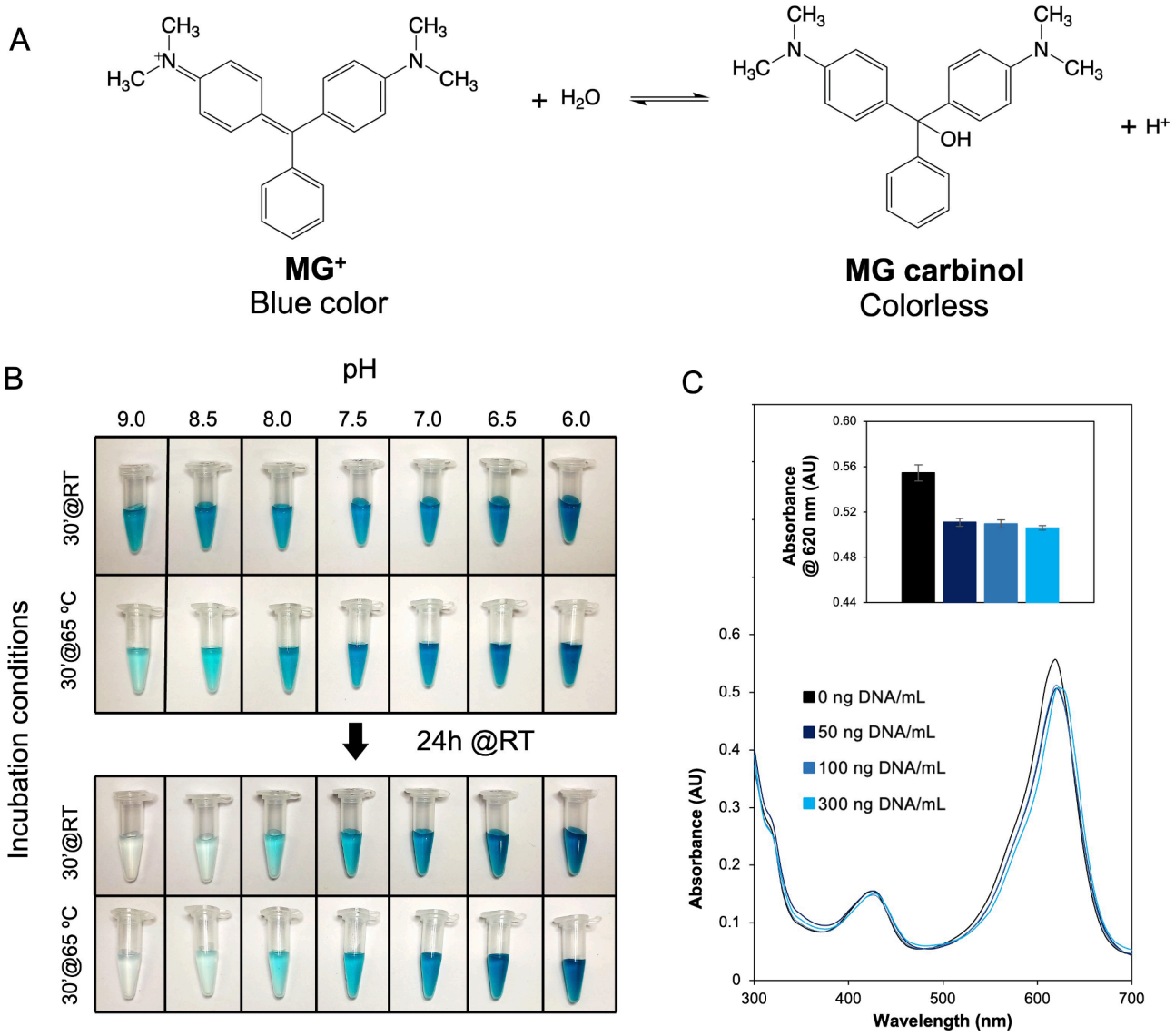

Fig. 1. Colorimetric behavior of MG in 0.1 M Tris-HCl buffer. A: Equilibrium of the two forms of MG in solution (pH > 3). B: pH effect on the color of MG solutions. Columns represent every pH studied, while rows refer to incubation conditions. C: DNA concentration effect on MG. Absorbance spectra with increasing concentrations of dsDNA are represented. Inset: Mean values of absorbance at 620 nm of MG in solutions with increasing concentrations of dsDNA. Error bars represent the standard deviation of three replicates. RT: Room temperature.

dsDNA on MG has been already described in Britton-Robinson buffers [19]. To assess if this behavior also occurs in Tris-HCl buffer, a 100 μM MG solution in Tris-HCl pH 7.5 buffer was prepared, and sheared salmon sperm DNA was added at different concentrations. Results can be observed in Fig. 1C and S1B, where the expected hypochromic effect, with a decrease in the absorbance at 620 nm, can be seen. Those values of absorbance at 620 nm show that, albeit a decrease in absorbance happens with the presence of dsDNA ($p < 7{\cdot}10^{-4}$ for all the cases), it does not change with concentration (from 50 to 300 ng/mL, $p > 0.1$ for all the cases). All results here presented confirm the hypothesis that both pH and DNA are key factors in the equilibrium of the MG forms present in LAMP reactions.

3.2. Malachite green in LAMP reactions: Electrochemical characterization

As the aim of this work is to present MG as an electrochemical probe for quantitative analysis, MG in solution was also characterized via electrochemical techniques. In this way, it could act as a dual visual (qualitative) / electrochemical (quantitative) indicator.

The first consideration when assessing MG as an electrochemical probe for LAMP reactions is the effect of the composition of the working buffer. Tris-HCl is the base buffer of LAMP, but LAMP mixes present other components, such as inorganic salts or surfactants that can affect the electrochemical signal. For this purpose, 100 μM MG solutions at pH 6.5, 7.5 and 8.5 were prepared in both Tris-HCl buffer and a commercial isothermal amplification buffer. CVs were recorded in both pH 7.5 buffer solutions in the potential window comprised between 0 and + 1.0 V (Fig. 2A). It can be clearly observed that MG presents in both buffers an intense and well-defined oxidation process (*Ia*, at 460 and 525 mV in Tris-HCl and isothermal amplification buffer, respectively), followed by a less intense process (*IIa*, at *ca.* 750 mV). These two processes have been previously described as the oxidation of the hydrated (*Ia*) and unhydrated (*IIa*) forms of MG [19]. A cathodic process appears at *ca.* 290 mV (*Ic*) with no significance from the analytical point of view. Thus, it seems that the amplification buffer does not contain relevant interferences, being appropriate for the use of MG as an electrochemical probe for LAMP detection. Therefore, all the following studies were performed in said buffer.

An ideal analytical signal should show a highly sensitive change with analyte concentration. Since while a LAMP reaction occurs, protons and pyrophosphate anions are released to the medium in a proportional manner with the number of initial copies of genetic material, a change in the electrochemical behavior of MG with pH should be observed. Thus, CVs were recorded in solutions of MG in LAMP buffer of different pH: 6.5, 7.5 and 8.5, covering the LAMP pH range (Fig. 2B). It can be clearly observed that the peak current intensity (I_p) of the first anodic process (*Ia*) decreases with pH. The peak potential (E_p) also moves towards more positive values, indicating that the electron transfer needs more energy to be produced. These changes could be used as analytical signals that correlate with the initial DNA copy number, at a given reaction time.

As mentioned before, the electrochemical behavior of MG regarding its interaction with DNA has been previously described in Britton-Robinson buffer. The DNA interaction with MG leads to a decrease in the diffusion coefficient of MG when bound to dsDNA, as well as a shift in the formal potential ($E^{o'}$) to more negative values [19]. To evaluate this behavior in LAMP buffer, different concentrations of sheared salmon sperm DNA were added to a 100 μM MG solution in isothermal amplification buffer (pH 7.5). It can be observed in Fig. 2C that, the more DNA present in the sample, the lower the I_p. A slight shift in peak potential can also be observed towards more negative values. With all these results, it can be concluded that the pH decrease and DNA synthesis lead to a decrease in I_p, that can be employed as analytical signal.

3.3. Evaluation of the presence of MG in commercial LAMP kits and its use as an electrochemical indicator for SARS-CoV-2 detection

Commercial kits use visual indicators for rapid assessment of negative/positive results. The Blue-LAMP RT Kit, with a characteristic shift from clear to light blue as LAMP progresses, was assessed for its direct electrochemical LAMP readout using SARS-CoV-2 RNA as a template. This LAMP kit was chosen as it presents a colorimetric behavior identical of that of MG, and thus a similar electrochemical behavior is expected given that the indicator in this kit is either MG or a very close derivative.

For this purpose, an initial RT-LAMP was carried out using a high copy number (4296 copies/μL). In Fig. 3A five replicates of LAMP reactions are shown together with five negative controls. After that, CVs were recorded for both negative and positive controls, showing a characteristic and intense oxidation peak at around 550 mV (Fig. 3A) that could correspond to the *Ia* MG process, as well as a small wave at around 820 mV, that could correspond to the *IIa*. The peak current intensity appears to decrease when comparing negative to positive samples (from 3.3 ± 0.17 μA to 2.2 ± 0.13 μA, $p = 4.3{\cdot}10^{-5}$), while the difference in peak potential was not significant (from 570 ± 10 mV to 560 ± 29 mV, $p = 0.92$). This decrease in peak current intensity can be explained by the already commented pH drop (Fig. 2B) and DNA synthesis (Fig. 2C). On the other hand, since E_p shifts to more positive values with lower pH and to more negative ones with increasing DNA concentration, the shift is negligible after LAMP reactions.

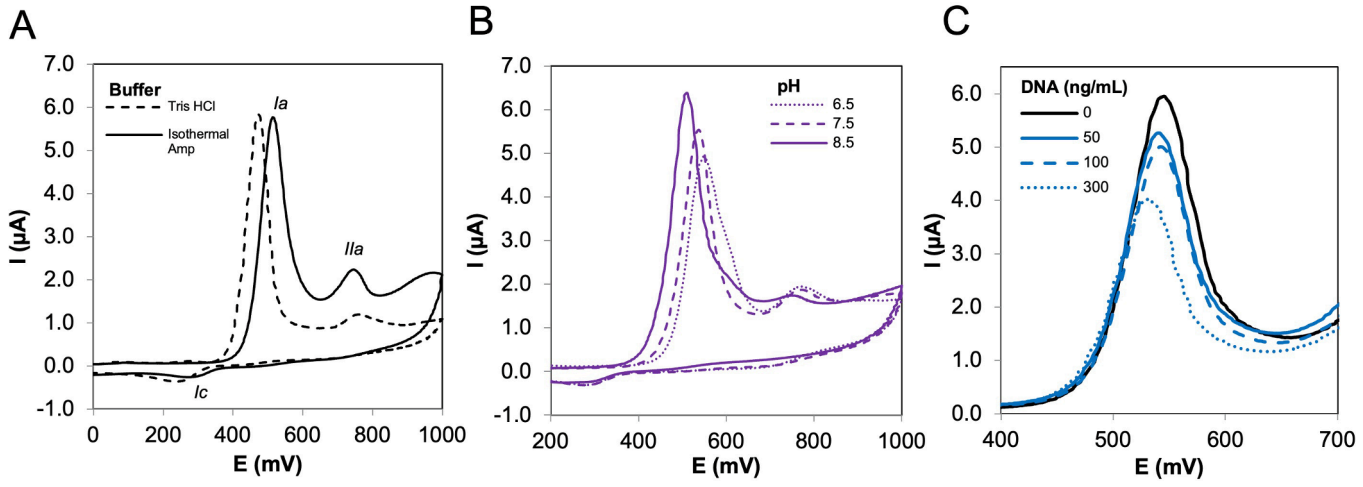

Fig. 2. Voltammograms recorded in 100 μM MG solutions in A: CVs using different buffer solutions at pH 7.5, B: CVs using LAMP buffer at different pH values. C: LSVs using LAMP buffer with different dsDNA concentrations (pH 7.5).

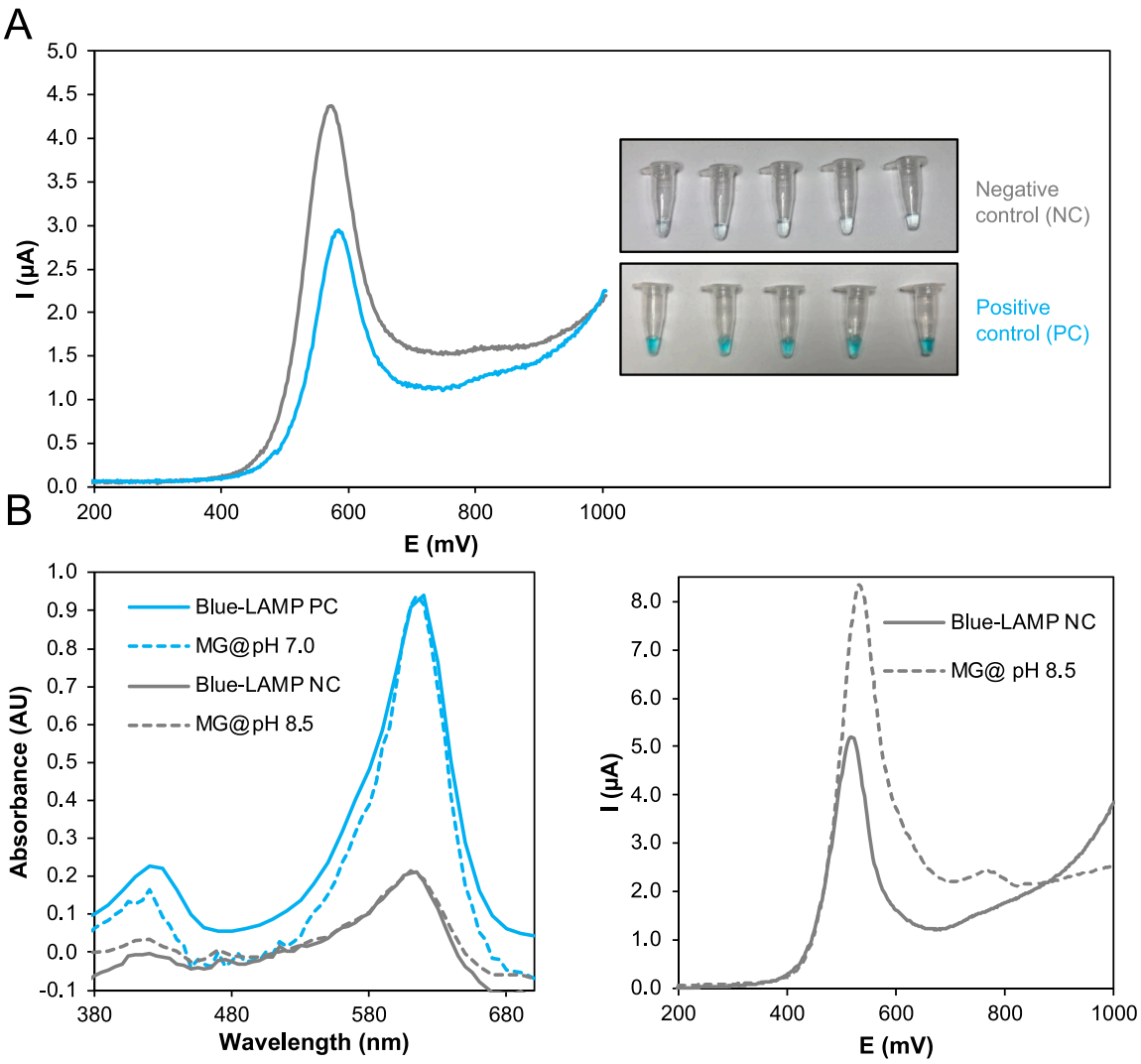

Fig. 3. A: Electrochemical characterization of the Blue-LAMP RT Kit. LSVs of one NC and one PC RT-LAMP reactions. Inset: Five replicates of both NC and PC. B: Analysis of the presence of MG in the Blue-LAMP RT Kit. Left: UV–Vis spectra of MG solutions at pH 8.5 and 7.0, and PC and NC of RT-LAMP. Right: CVs of an RT-LAMP buffer with 100 μM MG and Blue-LAMP RT Kit. Negative control (NC): no template; Positive control (PC): 4296 copies/μL of the N1 SARS-CoV-2 fragment. (For interpretation of the references to color in this figure legend, the reader is referred to the web version of this article.)

As this commercial LAMP kit presented a color shift equivalent to that of MG, the presence of said colorimetric indicator (or a derivative) could be deduced. To assess it, 100 μM MG solutions were prepared in isothermal amplification buffer of pH 8.5 and 7.0, to obtain both a blue and a colorless solution. These solutions were compared, using UV–Vis spectrophotometry, to positive and negative RT-LAMP reactions using the Blue-LAMP RT Kit (Fig. 3B left). The obtained spectra show an increase in the absorbance peak at 650 nm, when comparing negative reactions and MG@pH 8.5 (with a rather small peak) with positive reactions and MG@pH 7.0, with a clear increase in absorbance at the characteristic maximum of the cationic form of MG.

For further analysis, the commercial kit was also electrochemically assessed comparing the Blue-LAMP RT Kit with a 100 μM MG solution in isothermal amplification buffer. As can be seen in Fig. 3B right, the characteristic peak of the kit described in Fig. 3A also appears in the buffer where MG has been added, although with a higher peak current. These results confirm the presence of MG (or a molecule with a closely related structure and, in turn, with a similar electrochemical behavior) in the Blue-LAMP RT kit and in a concentration lower than 100 μM.

3.4. Electrochemical quantification of LAMP reactions using the commercial Blue-LAMP RT Kit

Once known the electrochemical behavior of MG and its presence in some commercial LAMP kits (either MG or a derivative [25]), the sensitivity and robustness of the analytical methodology using it as an electrochemical indicator in LAMP reactions was evaluated. Thus, a calibration curve of the RT-LAMP amplification of the N1 fragment of the SARS-CoV-2 genome, starting from different RNA concentrations, was performed. The change in color can be observed in Fig. 4A. LSVs recorded for the reactions showed that the peak current intensity correlated with the initial RNA concentration (Fig. S2). The corresponding calibration plot, shown in Fig. 4B, presents a good linear fit ($R^2 = 0.993$) with a sensitivity of 0.410 μA (per unit of increase in log [RNA]). It is important to note that the upper limit of the calibration curve is restricted due to the availability of SARS-CoV-2 RNA template, and if higher concentrations of RNA were tested, the calibration curve could be extended to higher concentrations (as the analysis of real samples suggests in the following section). A theoretical limit of detection (LOD) of 10 copies/μL, calculated as 3 times the standard deviation of the blank (negative control) divided by the slope of the linear fit, was obtained. However, we stablished a practical LOD of 22 copies/μL, based

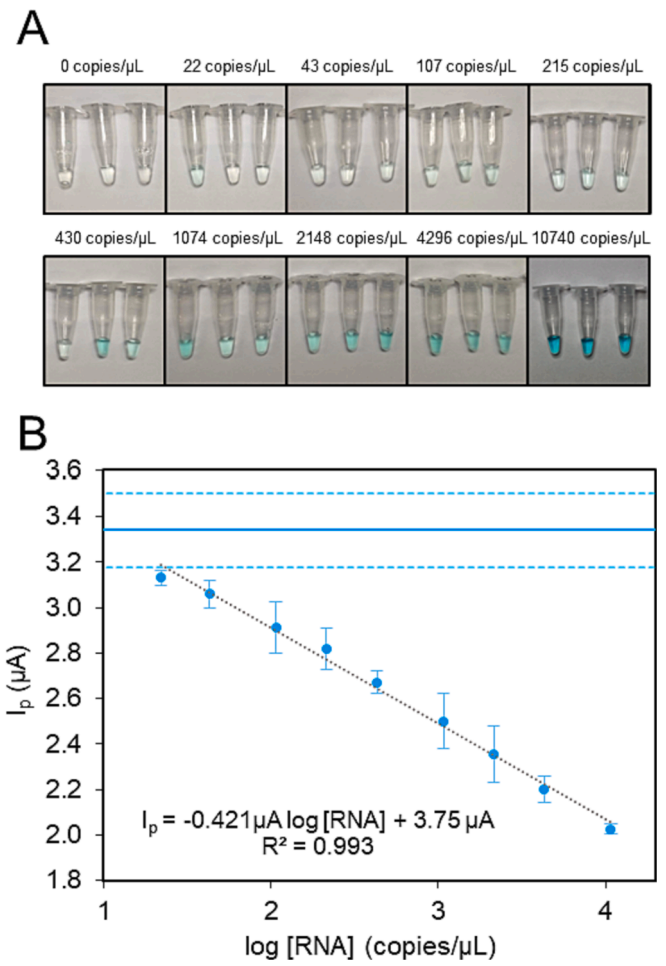

Fig. 4. Calibration plot obtained for the electrochemical determination of the N1 fragment of the SARS-CoV-2 genome using the Blue-LAMP RT KIT. A: Amplification results. B: Calibration plot with electrochemical measurements. Error bars represent the standard deviation of 4 replicates. The solid line indicates the mean value of non-template control samples (NC, 0 copies/µL). Dashed lines indicate 3 times the standard deviation of the NC. (For interpretation of the references to color in this figure legend, the reader is referred to the web version of this article.)

on the lowest discernible concentration.

It can be clearly appreciated how this electrochemical quantification approach improves the detection of the LAMP methodology. Visual readout provides an approximate and semiquantitative result, while the subsequent electrochemical measurement provides a precise quantification. For example, visual results shown in Fig. 4A would classify as negative the samples up to 215 copies/µL, while the difference between a sample with a copy number as low as 22 copies/µL can be clearly discerned from NC via electrochemical detection. Although this method shows a LOD slightly higher than other methods based on PCR [26] or on LAMP amplification using other electroactive indicators [27], the sensitivity here achieved is suitable for the diagnosis and monitoring of infectious diseases. Moreover, an easy procedure combined with simple instrumentation (miniaturized disposable electrochemical cells and portable potentiostat) would allow on-site confirmation of dubious samples, which is of enormous relevance for highly infective pathogens.

3.5. Application to real sample analysis

In order to prove the applicability of the method, 4 nasal swab samples from volunteering individuals were tested. Samples were collected at HUCA and RT-qPCR results were provided by the Clinical Laboratory of the Microbiology Unit. Samples 1 and 2 were classified as RT-qPCR negative, while samples 3 and 4 tested positive (Fig. S3). Our methodology coincided in the diagnosis, with negative samples presenting values under the limit of detection of the method. However, both positive samples presented peak current intensisites under the minimum present in the calibration curve (i.e., corresponding to a concentration higher than the highest tested, which is 10,740 copies/µL). Although both positive samples are out of the calibration range of our method, as can be seen in Fig. 5, the peak current intensity for sample 4 is lower than for sample 3, indicating that the initial number of copies is higher for sample 4, which is in accordance with the treshold cycle (Ct) results provided by routine PCR, as the Ct level of sample 3 was 28 and that of sample 4 was 18 (indicating a higher copy number in sample 4).

To prove the usefulness of the method in providing a quantitative result, dilutions of the samples were performed (Fig. 5). Thus, 1:5, 1:10 and 1:50 dilutions of samples 3 and 4 were analysed, with all dilutions of sample 3 falling within the linear range of the method, and only the highest dilution of sample 4 doing so. Taking this into account, sample 3 and 4 would contain $(2.5 \pm 0.2) \cdot 10^5$ and $(1.4 \pm 0.9) \cdot 10^7$ copies/µL, respectively, which is in accordance with routine PCR results mentioned before.

4. Conclusions

In this work, a simple, fast, and sensitive method for the electrochemical readout of LAMP reactions based on malachite green (a common LAMP indicator that turns blue when LAMP progresses) has been developed. The behavior of this electroactive indicator has been studied in different media, observing that, while pH and dsDNA promote a change in the MG equilibrium, temperature plays a key role in reaching the stable final form of MG in solution. The new approach here described adds to the visual detection of MG, the possibility of quantitation, and confirmation of dubious samples. The method has been applied to the determination of SARS-CoV-2 RNA, using the peak current intensity of the main anodic process of MG as the analytical signal that correlates with the initial number of copies of RNA. The method has been further validated with clinical samples from both healthy and COVID-19 patients.

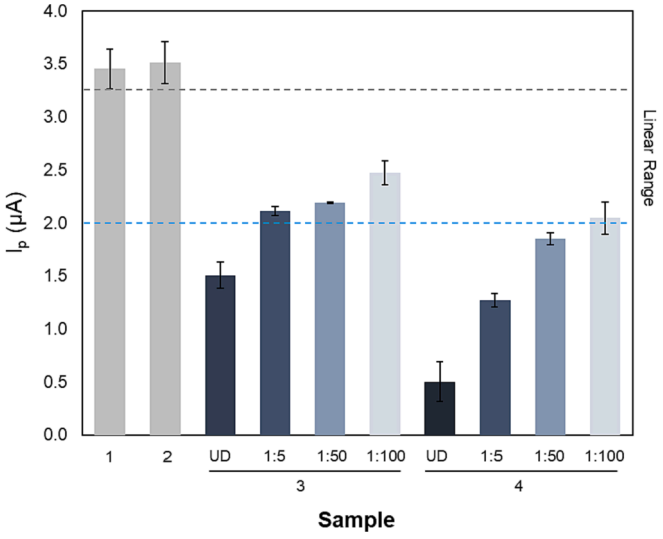

Fig. 5. Clinical sample analysis. Sample results are presented based on their peak current intensity (I_p). Samples 3 and 4 are indicated in terms of their dilution (UD: undiluted). The signals corresponding to the linear range are indicated by dashed lines, the corresponding to the upper limit of the linear range in blue and to the lower limit in grey. Error bars indicate the standard deviation of three replicates. (For interpretation of the references to color in this figure legend, the reader is referred to the web version of this article.)

This method employs a low-cost electrochemical detection system for the quantitation of LAMP reactions. Thus, we have demonstrated, as a proof-of-applicability, that this methodology could be the basis of the determination of SARS-CoV-2 using a commercial kit containing MG (or a MG-like indicator). Visual/electrochemical quali/quantitative detection could enable a first visual classification of samples (positive/unclear/negative) and, a subsequent electrochemical determination would inform about the copy number in the sample. This is a simple methodology that does not require extra reagents or complex equipment. However, this method still presents some of the limitations associated with this type of amplifications such as photosensitivity or possible carryover contamination. Thus, work is in progress to combine reaction and electrochemical detection into a simple electrochemical platform to obtain a fully integrated and field-deployable device.

CRediT authorship contribution statement

Pablo Rioboó-Legaspi: Conceptualization, Data curation, Formal analysis, Investigation, Writing – original draft, Visualization. **Noelia Rabanal-Rubio:** Formal analysis, Investigation, Writing – original draft. **Estefanía Costa-Rama:** Conceptualization, Funding acquisition, Methodology, Project administration, Supervision, Writing – review & editing, Visualization. **María Dolores Cima-Cabal:** Methodology, Writing – review & editing. **María del Mar García-Suárez:** Methodology, Writing – review & editing. **M. Teresa Fernández-Abedul:** Conceptualization, Methodology, Supervision, Visualization, Writing – review & editing, Funding acquisition.

Declaration of competing interest

The authors declare the following financial interests/personal relationships which may be considered as potential competing interests: M.T.F.-A. declares she was one of the founders of Micrux Technologies, a company engaged in the development of miniaturized electrodes and electrochemical/microfluidic equipment and remains a consultant and shareholder. She declares it has not influenced the work reported in this paper. The rest of authors declare no competing financial interest.

Data availability

Data will be made available on request.

Acknowledgments

This work has been supported the I + D + I project PID2020-118376RA-I00 funded by MCIN/AEI/10.13039/501100011033, the PCTI Program of the Government of the Principality of Asturias and FEDER Program of the European Union (AYUD/2021/51289) and the project LIFE of the Fondo Supera COVID-19 from Banco de Santander, CRUE and CSIC. P.R.L. thanks for the support of the grant "Severo Ochoa" (BP21-029) funded by the Asturian Council for Science, Technology, and Innovation. E.C.R. thanks for the support of the grant "Beatriz Galindo" (BG20/00027) funded by the Ministry of Universities of the Spanish Government. Authors would like to acknowledge the technical support from Servicios Científico-Técnicos of the University of Oviedo and the Service of Microbiology and Emergency Care of the HUCA.

Appendix A. Supplementary data

Supplementary data to this article can be found online at https://doi.org/10.1016/j.microc.2024.110172.

References

[1] D. Das, C.-W. Lin, H.-S. Chuang, LAMP-based point-of-care biosensors for rapid pathogen detection, Biosensors. 12 (2022) 1068, https://doi.org/10.3390/bios12121068.
[2] A. Ainla, M.P.S. Mousavi, M.-N. Tsaloglou, J. Redston, J.G. Bell, M.T. Fernandez-Abedul, G.M. Whitesides, Open-source potentiostat for wireless electrochemical detection with smartphones, Anal. Chem. 90 (2018) 6240–6246, https://doi.org/10.1021/acs.analchem.8b00850.
[3] A. Nemiroski, D.C. Christodouleas, J.W. Hennek, A.A. Kumar, E.J. Maxwell, M. T. Fernandez-Abedul, G.M. Whitesides, A universal Mobile electrochemical detector designed for use in resource-limited applications, Proc. Natl. Acad. Sci. USA 111 (2014) 11984–11989, https://doi.org/10.1073/pnas.1405679111.
[4] G. Xiang, X. Pu, D. Jiang, L. Liu, C. Liu, X. Liu, Development of a real-time resistance measurement for Vibrio parahaemolyticus detection by the lecithin-dependent hemolysin gene, PLoS One. 8 (2013) e72342, https://doi.org/10.1371/journal.pone.0072342.
[5] H. Kong, W. Zhang, J. Yao, C. Li, R. Lu, Z. Guo, J. Li, C. Li, Y. Li, C. Zhang, L. Zhou, A RT-LAMP based hydrogen ion selective electrode sensing for effective detection HIV-1 RNA with high-sensitivity, Sens. Actuators B Chem. 329 (2021) 129118, https://doi.org/10.1016/j.snb.2020.129118.
[6] Z. Xu, K. Yin, X. Ding, Z. Li, X. Sun, B. Li, R.V. Lalla, R. Gross, C. Liu, An integrated E-tube cap for sample preparation, isothermal amplification and label-free electrochemical detection of DNA, Biosens. Bioelectron. 186 (2021) 113306, https://doi.org/10.1016/j.bios.2021.113306.
[7] A. Rodríguez-Penedo, P. Rioboó-Legaspi, A. González-López, A. Lores-Padín, R. Pereiro, M.M. García-Suárez, M.D. Cima-Cabal, E. Costa-Rama, B. Fernández, M. T. Fernández-Abedul, Electrocatalytic palladium nanoclusters as versatile indicators of bioassays: rapid electroanalytical detection of SARS-CoV-2 by reverse transcriptase isothermal loop-mediated amplification, Adv. Healthc. Mater. (2023) 2202972, https://doi.org/10.1002/adhm.202202972.
[8] W. Jaroenram, J. Kampeera, N. Arunrut, C. Karuwan, A. Sappat, P. Khumwan, S. Jaitrong, K. Boonnak, T. Prammananan, A. Chaiprasert, A. Tuantranont, W. Kiatpathomchai, Graphene-based electrochemical genosensor incorporated loop-mediated isothermal amplification for rapid on-site detection of *Mycobacterium tuberculosis*, J. Pharm. Biomed. Anal. 186 (2020) 113333, https://doi.org/10.1016/j.jpba.2020.113333.
[9] A. Rivas-Macho, U. Eletxigerra, R. Diez-Ahedo, S. Merino, A. Sanjuan, M.M. Bou-Ali, L. Ruiz-Rubio, J. del Campo, J.L. Vilas-Vilela, F. Goñi-de-Cerio, G. Olabarria, Design and 3D printing of an electrochemical sensor for listeria monocytogenes detection based on loop mediated isothermal amplification, Heliyon 9 (2023) e12637, https://doi.org/10.1016/j.heliyon.2022.e12637.
[10] K. Hashimoto, M. Inada, K. Ito, Multiplex real-time loop-mediated isothermal amplification using an electrochemical DNA Chip consisting of a single liquid-Flow Channel, Anal. Chem. 91 (2019) 3227–3232, https://doi.org/10.1021/acs.analchem.8b05284.
[11] J. Gao, C. Yang, X. Wu, W. Huang, J. Ye, R. Yuan, W. Xu, A highly sensitive electrochemical biosensor via short-stranded DNA activating LAMP(H+) to regulate i-motif folds for signal transduction, Sens. Actuators B Chem. 380 (2023) 133354, https://doi.org/10.1016/j.snb.2023.133354.
[12] A.S. Patterson, D.M. Heithoff, B.S. Ferguson, H. Tom Soh, M.J. Mahan, K. W. Plaxco, Microfluidic chip-based detection and intraspecies strain discrimination of *Salmonella* serovars derived from whole blood of septic mice, Appl. Environ. Microbiol. 79 (2013) 2302–2311, https://doi.org/10.1128/AEM.03882-12.
[13] N.W. Lucchi, D. Ljolje, L. Silva-Flannery, V. Udhayakumar, Use of malachite green-loop mediated isothermal amplification for detection of *Plasmodium* spp. parasites, PLoS One. 11 (2016) e0151437, https://doi.org/10.1371/journal.pone.0151437.
[14] J. Gachugia, W. Chebore, K. Otieno, C.W. Ngugi, A. Godana, S. Kariuki, Evaluation of the colorimetric malachite green loop-mediated isothermal amplification (MG-LAMP) assay for the detection of malaria species at two different health facilities in a malaria endemic area of western Kenya, Malar. J. 19 (2020) 329, https://doi.org/10.1186/s12936-020-03397-0.
[15] K.A. Barazorda, C.J. Salas, D.K. Bishop, N. Lucchi, H.O. Valdivia, Comparison of real time and malachite-green based loop-mediated isothermal amplification assays for the detection of plasmodium vivax and P. falciparum, PLoS One. 15 (2020) e0234263-, https://doi.org/10.1371/journal.pone.0234263.
[16] A. Martín Ramírez, M. Suárez, C. García, S. Hisam, A. Perez-Ayala, J. Rubio, Usefulness of malachite-green LAMP for diagnosis of plasmodium and five human malaria species in a nonendemic setting, Am. J. Trop. Med. Hyg. 106 (2022) 1414–1420, https://doi.org/10.4269/ajtmh.21-1151.
[17] M.M. Bordbar, H. Samadinia, A. Hajian, A. Sheini, E. Safaei, J. Aboonajmi, F. Arduini, H. Sharghi, P. Hashemi, H. Khoshsafar, M. Ghanei, H. Bagheri, Mask assistance to colorimetric sniffers for detection of Covid-19 disease using exhaled breath metabolites, Sens. Actuators B Chem. 369 (2022) 132379, https://doi.org/10.1016/j.snb.2022.132379.
[18] C.J. Cooksey, Quirks of dye nomenclature. 6. malachite green, Biotechnic & Histochemistry. 91 (2016) 438–444, https://doi.org/10.1080/10520295.2016.1209787.
[19] X. Hu, K. Jiao, W. Sun, J.-Y. You, Electrochemical and spectroscopic studies on the interaction of malachite green with DNA and its application, Electroanalysis. 18 (2006) 613–620, https://doi.org/10.1002/elan.200503438.
[20] W.E. Huang, B. Lim, C.-C. Hsu, D. Xiong, W. Wu, Y. Yu, H. Jia, Y. Wang, Y. Zeng, M. Ji, H. Chang, X. Zhang, H. Wang, Z. Cui, RT-LAMP for rapid diagnosis of coronavirus SARS-CoV-2. Microb. Biotechnol. 13 (2020) 950–961, https://doi.org/10.1111/1751-7915.13586.

[21] C. Batéjat, Q. Grassin, J.-C. Manuguerra, I. Leclercq, Heat inactivation of the severe acute respiratory syndrome coronavirus 2, J. Biosaf. Biosecur. 3 (2021) 1–3, https://doi.org/10.1016/j.jobb.2020.12.001.

[22] A.R. Fischer, P. Werner, K.U. Goss, Photodegradation of malachite green and malachite green carbinol under irradiation with different wavelength ranges, Chemosphere. 82 (2011) 210–214, https://doi.org/10.1016/J.CHEMOSPHERE.2010.10.019.

[23] M.C. Nguyen, I. Shoji, K. Noboru, Donnan electric potential dependence of intraparticle diffusion of malachite green in single cation exchange resin particles: a laser trapping-microspectroscopy study, Am. J. Analyt. Chem. 2012 (2012) 188–194, https://doi.org/10.4236/AJAC.2012.33027.

[24] R.J. Goldacre, J.N. Phillips, 370. the ionization of basic triphenylmethane dyes, J. Chem. Soc. (1949) 1724–1732, https://doi.org/10.1039/JR9490001724.

[25] J. Lux, E.J. Peña, F. Bolze, M. Heinlein, J.F. Nicoud, Malachite green derivatives for two-photon RNA detection, ChemBioChem. 13 (2012) 1206–1213, https://doi.org/10.1002/CBIC.201100747.

[26] D. Dutta, S. Naiyer, S. Mansuri, N. Soni, V. Singh, K.H. Bhat, N. Singh, G. Arora, M. S. Mansuri, COVID-19 diagnosis: a comprehensive review of the RT-qPCR method for detection of SARS-CoV-2, Diagnostics 12 (2022) 1503, https://doi.org/10.3390/diagnostics12061503.

[27] P. Rioboó-Legaspi, A. González-López, J.F. Beltrán-Sánchez, M.D. Cima-Cabal, M. M. García-Suárez, A.J.G. Sánchez, T. Fernández-Otero, J.G. Haro, E. Costa-Rama, M.T. Fernández-Abedul, Phenol red as electrochemical indicator for highly sensitive quantification of SARS-CoV-2 by loop-mediated isothermal amplification detection, Talanta. (2023) 124963, https://doi.org/10.1016/j.talanta.2023.124963.